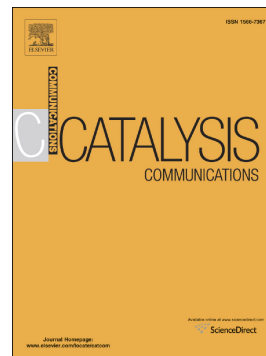


Accepted Manuscript

Gas-phase conversion of glycerol to allyl alcohol over vanadium-supported zeolite beta

Ruben Almeida, M. Filipa Ribeiro, Auguste Fernandes, João P. Lourenço



PII: S1566-7367(19)30129-3
DOI: <https://doi.org/10.1016/j.catcom.2019.04.015>
Reference: CATCOM 5683
To appear in: *Catalysis Communications*
Received date: 17 January 2019
Revised date: 10 April 2019
Accepted date: 20 April 2019

Please cite this article as: R. Almeida, M.F. Ribeiro, A. Fernandes, et al., Gas-phase conversion of glycerol to allyl alcohol over vanadium-supported zeolite beta, *Catalysis Communications*, <https://doi.org/10.1016/j.catcom.2019.04.015>

This is a PDF file of an unedited manuscript that has been accepted for publication. As a service to our customers we are providing this early version of the manuscript. The manuscript will undergo copyediting, typesetting, and review of the resulting proof before it is published in its final form. Please note that during the production process errors may be discovered which could affect the content, and all legal disclaimers that apply to the journal pertain.

Gas-phase conversion of glycerol to allyl alcohol over vanadium-supported zeolite beta

Ruben Almeida^a, M. Filipa Ribeiro^b Auguste Fernandes^{b,*} jlouren@ualg.pt, João P. Lourenço^{a,b,*} jlouren@ualg.pt

^aFaculdade de Ciências e Tecnologia, CIQA, Universidade do Algarve, Campus de Gambelas, 8005-139 Faro, Portugal

^bCentro de Química Estrutural, Instituto Superior Técnico, Universidade de Lisboa, Av. Rovisco Pais, 1049-001 Lisboa, Portugal

*Corresponding authors.

ACCEPTED MANUSCRIPT

Abstract

Vanadium oxide supported beta zeolite (Si/Al=25, 4% V) was used as catalyst for the one-pot gas-phase conversion of glycerol to allyl alcohol without any external reductant. The catalytic data strongly suggest a consecutive reactions path involving the dehydration to acrolein over the zeolite acid sites followed by a selective reduction through a hydrogen-transfer reaction. Acidity is expected to play a major role in what concerns the selectivity, as demonstrated by the catalytic results obtained by the impregnation of vanadium on a previously Cs-exchanged sample that achieved ca. 30% selectivity to allyl alcohol at ca. 20% glycerol conversion.

Keywords: Allyl alcohol, Vanadium oxide, Glycerol conversion, Beta zeolite, Sustainable chemistry

1. Introduction

Glycerol, a polyalcohol readily obtained from biomass, is a chemical product with wide applications in pharmaceutical, cosmetic and food industries. This compound is found in association with fatty acids forming triglycerides and it is consequently produced as a by-product in the soap and biodiesel industries. In the last years, the continuous demand for more sustainable alternatives to fossil fuels, including biodiesel, has led to a surplus of glycerol production that tends to reduce its market price. The conversion of glycerol into value-added commodity chemicals and fuels is, thus, of paramount importance to improve the biodiesel economic viability [1–3].

The gas-phase catalytic dehydration to acrolein is one of the most studied ways for the valorisation of glycerol. Acrolein is mainly used for the production of acrylic acid, acrylic acid esters, superabsorber polymers and detergents [4,5]. A large variety of acid catalysts has been reported for this reaction, including zeolites, heteropolyacids, metal oxides and modified mesoporous silica materials [6–13], with their acid and textural properties playing a crucial role on the catalytic performance [11,14–16].

A less explored way for the valorization of glycerol is its direct conversion to allyl alcohol, an important chemical intermediate due to the presence of C=C and O-H functionalities. Allyl alcohol derivatives can be found in cosmetic, pharmaceutical and food industries and are also a building block in the manufacture of various chemical compounds such as coupling agents, plasticizers, crosslinking agents and coating additives [17]. The production of allyl alcohol currently involves the conversion of propylene, however, a few reports have shown that it can be obtained in a one-pot reaction from glycerol, using zirconia-iron [18], $\text{MoO}_3\text{-WO}_3/\text{TiO}_2$ [19] and methyltrioxorhenium (MTO) [20]. Recently, G. Sánchez et al. [17,21] used ZSM-5 and alumina supported iron catalysts for this purpose, taking advantage of the support acidity to dehydrate the glycerol and the iron species to promote the formation of allyl alcohol through an hydrogen transfer reaction that may involve chemical intermediates from the dehydration. These works reveal important insights on the mechanism of this reaction but also demonstrate that improvement of the catalyst is still needed in order to increase the selectivity to allyl alcohol.

Vanadium compounds supported on zeolites have proved to be successful catalysts for the conversion of glycerol to acrylic acid [22]. To the best of our knowledge, these bifunctional catalysts have never been tested in the direct conversion of glycerol to allyl alcohol, although NH_4VO_3 was shown to be active in liquid phase [23]. In this work, we intend to evaluate the

ability of vanadium oxide supported on beta zeolite and its modification with cesium (in order to control the acidity) as catalysts for the one-pass conversion of glycerol to allyl alcohol and to demonstrate that redox phases other than iron oxide, could be considered for this catalytic system.

2. Experimental

2.1. Catalyst preparation

Beta zeolite in the protonic form (VALFOR CP811BL-25, Si/Al ratio of 25) was purchased from *The PQ Corporation* (USA). A sample of V-containing beta zeolite (BEA/V) was prepared by a procedure following closely that described by L.G. Possato et al. [22]. Briefly, 1.0 g of zeolite was stirred with the required amount of an aqueous solution of NH_4VO_3 (0.04 mol.L^{-1}) at room temperature for 2 h. The water was removed in a rotary evaporator followed by a calcination at $500 \text{ }^\circ\text{C}$ under dry air for 2 h. The sample prepared by this procedure was named BEA/V.

In order to evaluate the effect of the modification with cesium ions, a sample (BEA/Cs/V) was obtained by first ion-exchanging the beta zeolite with a 0.1 M aqueous solution of CsCl for 2 h at $80 \text{ }^\circ\text{C}$. The powder recovered after filtration was dried at $80 \text{ }^\circ\text{C}$ overnight, calcined under dry air for 1 h, at $350 \text{ }^\circ\text{C}$, and subsequently submitted to the vanadium deposition as described above.

2.2 Catalyst characterization

Powder X-ray diffraction patterns were recorded on a Panalytical X'Pert Pro diffractometer using Cu $K\alpha$ radiation filtered by Ni and an X'Celerator detector. Phase identification was carried out using the Panalytical software and the ICDD PDF2 database. Pyridine (Py) adsorption was followed by FTIR spectroscopy using a home-made quartz cell allowing sample vacuum (10^{-6} Torr) and temperature pretreatment ($450 \text{ }^\circ\text{C}$, 2h) and subsequent Py adsorption at $150 \text{ }^\circ\text{C}$. Quantitative measurements were done as described elsewhere [24]. Thermogravimetric data (TG) were obtained with a Setsys Evo15 Setaram apparatus, under air at a heating rate of $10 \text{ }^\circ\text{C.min}^{-1}$. Nitrogen sorption experiments were carried out using an

Autosorb IQ series equipment from Quantachrome. Prior to measurements, the samples were outgassed first at 90 °C and then at 350 °C, during 1 and 4 h, respectively.

UV-Visible spectra were recorded with a high temperature reaction cell from Harrick and a Praying Mantis diffuse reflectance accessory, both coupled to a Cary 5000 spectrophotometer from Varian.

The amount of supported Cs and V was determined by bulk chemical analysis using AA and ICP-OES techniques.

2.3. Catalytic tests

Conversion of glycerol was carried out at 320 °C under atmospheric pressure, in a fixed-bed flow type quartz reactor (i.d. 1.5 cm) using 150 mg of catalyst. Before each test, the catalyst was maintained for 1 h at 500 °C under a flux of dry air (30 mL·min⁻¹). The reaction feed, an aqueous solution containing 10 wt.% of glycerol, was introduced into the reactor by a syringe pump KD Scientific at a flow of 2.5 mL·h⁻¹ and diluted in a flow of dry nitrogen (30 mL·min⁻¹). The reaction products were collected in an ice trap followed by two additional water traps. The reaction products were analyzed on a Bruker SCION 460 gas chromatograph equipped with a 30 m Zebron ZE-FFAP capillary column and a FID detector. For quantitative measurements, 1-propanol (for low boiling point products) and 1,4-butanediol (for glycerol) were used as internal standards. Since 1-propanol is a possible reaction product, the samples were also checked for the presence of this compound.

The conversion and selectivity were calculated as follows:

$$\% \text{ Conv} = \frac{n_{g_{total}} - n_{g_t}}{n_{g_{total}}} \times 100$$

$$\% \text{ Sel}_i = \frac{n_{g_{i,t}}}{n_{g_{total}} - n_{g_t}} \times 100$$

where $n_{g_{total}}$ is the total number of moles of glycerol injected into the reactor during the time on stream t , n_{g_t} the number of moles of glycerol in the products recovered at time on stream t and $n_{g_{i,t}}$ the number of moles of glycerol converted to the product i during the time on stream t . In order to obtain a significant amount of products, each analysis corresponds to the products recovered for 2 h.

3. Results and discussion

The XRD patterns of calcined samples (figure SD1) are those of typical beta zeolite. The deposition of vanadium does not significantly damage the structure of the parent beta zeolite, although a decrease in the crystallinity can be observed in the modified samples. The presence of crystalline V-containing phases could not be clearly identified although the presence of small and disperse vanadium oxides cannot be discarded when the patterns are compared with the ICDD cards #01-074-1595 (V_2O_5) and #01-070-2717 (VO_2).

The chemical, acidic and textural properties of the various samples are shown in table 1. The deposition of vanadium and subsequent calcination gives rise to a decrease of the surface area and micropore volume (samples BEA and BEA/V) probably due to some pore blockage, although a damage of the structure cannot be ruled out taking into consideration the reduction of crystallinity observed by XRD. The sample containing cesium and vanadium, although showing a further decrease, still retains a high BET surface area and micropore volume.

The UV-Vis. spectra (figure 1) display bands at ca. 260 and 400 nm that overlap, at least, with one band at ca. 300-310 nm, all corresponding to oxygen to V charge-transfer bands. The absence of bands in the range 600-800 nm, characteristic of d-d transitions of V^{4+} species, indicates that all the vanadium atoms are in oxidation state (+5) [25]. The band near 400 nm has been assigned to polymeric octahedral V^{5+} [25] whereas the band at ca. 260 and 300-310 nm were associated to monomeric and oligomeric tetrahedral V^{5+} [26], respectively. Although no crystalline V_2O_5 could be indubitably observed, the presence of highly dispersed V_2O_5 cannot be discarded. As shown by M. Wark et al. [27], highly dispersed V_2O_5 gives rise to a significantly different spectrum where a monotonic increase of absorption up to a maximum at ca. 220 nm is observed, instead of the typical bands of the crystalline phase. Moreover, preliminary results obtained with Raman spectroscopy indicate the presence of V_2O_5 in these samples.

The catalytic performance of the various samples concerning the conversion of glycerol is depicted in figure 2. Under the conditions of the present study, a strong deactivation is observed in the first hours on stream for all the samples, as expected for acidic zeolites [28]. This deactivation is usually explained by the formation of coke, which depends on the number and strength of the acid sites [29]. From table 1 (and figure SD2), it is evident that the sample BEA/Cs/V has a much lower number of acid sites than the other samples and, consequently, it would be expected a significantly lower activity from the early stages of the reaction run. Nevertheless, it is observed that the initial conversion of glycerol is similar to those obtained

with the higher acidic samples. This result suggests that neither strong acid sites nor a high density of acid sites are needed to promote the conversion of glycerol in these conditions. The strong deactivation rate observed for all the samples, albeit having different acidity, may be explained by the different amount and type of coke that is formed. Table SD1 shows that the amount of coke correlates with the acidity of the samples and the DSC profiles (figure 4) show two exothermic peaks usually observed during the oxidation of coke on microporous catalysts: one appearing at low temperature, corresponding to the oxidation of less condensed coke (soft-coke), and the other at high temperature corresponding to more condensed coke (hard-coke) [15]. Although less visible in the TG profiles of the samples BEA and BEA/V, BEA/Cs/V shows two well differentiated weight losses in the range 300-600 °C, corresponding to these two types of coke (see figure SD 3).

Comparing the three samples, those containing V show both maxima at temperatures considerably lower than those observed for the BEA sample, certainly due to the ability of V-species to act as catalysts in the process of the coke oxidation. BEA, the sample that has stronger acid sites, gives rise to a higher amount of coke (24.5 wt.%, table SD1) and to a more condensed coke (figure 4) which causes a strong deactivation. On the other hand, the less acidic sample (BEA/Cs/V) gives rise to the lowest amount (20.0 wt.%, table SD1) and less condensed coke but this coke could be also effective in the deactivation of the catalyst due to the low initial number of acid sites. BEA/V shows an intermediate behavior, both in terms of the amount and nature of coke, as expected from its intermediate acidity.

For BEA catalyst under a 24 h catalytic test, the main reaction products were, as expected [28], acrolein, acetaldehyde and hydroxyacetone, with a minor amount of allyl alcohol and propionic aldehyde (figure 3). It should be noted that the selectivity of allyl alcohol never exceeds 2 % in these conditions.

The modification with vanadium (sample BEA/V) causes some significant changes in the product distribution (figure 5 A). Acrolein is again the main product but with a higher selectivity, whereas the selectivity to hydroxyacetone has been substantially reduced. These variations are probably related with the decrease of the number of both Lewis and Brönsted acid sites [12] in the BEA/V sample. Additionally, it is also important to note the increase of the selectivity to allyl alcohol, that reaches up to ca. 7 %. This result clearly indicates the ability of the vanadium species to promote reactions leading to the formation of allyl alcohol.

In order to investigate the influence of the support acidity on the formation of allyl alcohol, we prepared a new V-supported sample by previously exchanging the parent beta zeolite with

Cs ions (sample BEA/Cs/V). In this case, it was possible to obtain up to 30 % selectivity to allyl alcohol alongside with a decrease of the selectivity to acrolein (figure 5 B). A similar behaviour was already observed by G. Sánchez et al. [17] with iron supported ZSM-5 catalysts modified with rubidium. Using 13 % Fe supported on ZSM-5 at 340 °C and a GHSV of 1240 h⁻¹, those authors reported an increase of allyl alcohol yield from ca. 6 % to ca. 12 % when the catalyst was modified with Rb. The decrease in the acidity, particularly the reduction of the strongest acid sites, was found to play an important role in the catalytic behavior of the tested samples. Although the ion-exchange with Cs ions causes an evident reduction of the number of acid sites that may account for the change in the selectivity, it also introduces some basicity to the catalyst [30] that could play a role in the catalytic process and, thus, a comprehensive study involving other cations is in progress in order to clarify this point. Although the direct comparison with other published studies is rather difficult due to the different conditions used, the results reported here compare fairly with those reported for this catalytic process using related catalysts. The highest yield of allyl alcohol obtained with the sample BEA/Cs/V, ca. 10.5 % after 4 h on stream (figure SD4), is slightly lower than that found by G. Sánchez et al. using ZSM-5/Fe/Rb [17] or γ -alumina/Fe/Rb [21] catalysts (11.9 and 11.6 %, respectively), but it was obtained with a lower amount of metal phase and also at lower temperature. Higher temperature (400 °C) and high hydrogen pressure was also needed in other reported study to obtain allyl alcohol selectivity of ca. 20 % [31]. Therefore, while there is room for improvement regarding the catalytic activity and deactivation (that may influence the selectivity), the results reported in the present manuscript for V/zeolite-based catalysts are very promising and worthy of further investigation.

The mechanism for the formation of allyl alcohol from glycerol with metallic-based catalysts, in absence of molecular hydrogen, is not entirely clear and seems to depend on the catalyst. Y. Liu et al. [32], using an iron oxide catalyst, concluded that this process comprises the dehydration of glycerol to acrolein, followed by acrolein reduction to allyl alcohol, through an hydrogen transfer. Those authors carried out a comprehensive study with different alcohols as H-donors and observed that the best results were obtained with glycerol, although this reaction could also occur with other alcohols. In that study, the authors also concluded that intermediates with hydroxy groups formed during the reaction may participate together with glycerol as H-donors. On the other hand, J. Yi et al. [20] working with rhenium compounds identified a pathway not involving acrolein. In this case, allyl alcohol formation involves a rhenium diolate and a H-transfer from a second molecule of glycerol. A similar mechanism

was recently identified by A. R. Petersen et al. [23] who conducted a liquid phase comprehensive study using NH_4VO_3 as catalyst and deuterium-labelled glycerol, in order to elucidate the role of glycerol in the formation of allyl alcohol.

In the present work, both BEA/V and Cs/BEA/V seem to contain the same vanadium species, but show a rather different behavior in what concerns the selectivity towards allyl alcohol. Although the mechanism identified by J. Yi et al. and A. R. Petersen et al. [20,23] (which only requires the presence of the metal centre) cannot be discarded, the different behavior of the two samples (with similar vanadium content) suggests that a pathway involving just the vanadium species is not the main route for the conversion of glycerol to allyl alcohol in the present conditions. On the other hand, taking into consideration that the selectivity to acrolein tends to increase with the decrease of the acidity, it would be expected a higher selectivity towards this compound for the sample Cs/BEA/V when compared with the sample BEA/V, but we observe, instead, a reduction of the selectivity to acrolein and a significant increase of the selectivity to allyl alcohol. This result strongly suggests that the allyl alcohol is mainly formed at expenses of acrolein as reported by Y. Liu et al. [32] (see scheme SD1). In an analogous way, Pérez-Ramírez and coworkers [31] working in gas phase and using hydrogen as reductant, have shown that supporting silver on a hierarchical HZSM-5 zeolite allows the formation of allylic alcohol via the reduction of acrolein formed on the acid sites of the catalyst. In the present case, no molecular hydrogen is provided and the reduction of acrolein may be accomplished by hydrogen transfer reactions. Further studies are in progress in our research group in order to shed some light on the role of the acidity and on the different reactions involved in the mechanism.

Zeolites are well known for their structural stability and ability to support regeneration procedures at medium to high temperatures. In order to assess the reusability of the catalysts used in this study, a regeneration of the spent BEA/Cs/V sample was carried out at 530 °C for 10 h, under a flow of dry air. Results show that structural integrity is retained and the catalyst recovers its initial catalytic performance (Figures SD5 and SD6).

4. Conclusion

The present study clearly demonstrate that beta zeolite modified with vanadium oxide, already known to act as oxidation catalyst, is also able to promote the one-pass conversion of glycerol to allyl alcohol in absence of an additional reductant. A significant selectivity to allyl alcohol can be achieved by an appropriate tuning of the acidity through the ion-exchange of

the parent zeolite with Cs. The data reported here put in evidence the potential of this catalyst and make it worthy of detailed investigation. The significant deactivation of the catalyst is the main drawback and a further optimization in terms of zeolite structure, vanadium loading and operation conditions is needed in order to reduce deactivation and improve selectivity.

Acknowledgements

The authors thank Fundação para a Ciência e Tecnologia (FCT), Portugal, for financial support through the projects UID/QUI/00100/2019 and PEst-OE/QUI/UI4023/2014. A. Fernandes is grateful for FCT contract (from law DL/57).

References

- [1] M. Pagliaro, M. Rossi, *The Future of Glycerol*, second ed. RSC Publishing, Cambridge, 2010 ISBN: 978-1-84973-046-4.
- [2] C.A.G. Quispe, C.J.R. Coronado, J.A. Carvalho Jr., *Renew. Sustain. Energy Rev.* 27 (2013) 475–493.
- [3] A. Galadima, O. Muraza, *J. Taiwan Inst. Chem. Eng.* 67 (2016) 29–44.
- [4] M. Pagliaro, R. Ciriminna, H. Kimura, M. Rossi, C. Della Pina, *Angew. Chemie - Int. Ed.* 46 (2007) 4434–4440.
- [5] B. Katryniok, S. Paul, V. Bellière-Baca, P. Rey, F. Dumeignil, *Green Chem.* 12 (2010) 2079.
- [6] Y.T. Kim, K.D. Jung, E.D. Park, *Appl. Catal. A Gen.* 393 (2011) 275–287.
- [7] J.P. Lourenço, A. Fernandes, R.A. Bértolo, M.F. Ribeiro, *RSC Adv.* 5 (2015) 10667–10674.
- [8] A. Corma, G.W. Huber, L. Sauvanaud, P. O'Connor, *J. Catal.* 257 (2008) 163–171.
- [9] A. Alhanash, E.F. Kozhevnikova, I. V. Kozhevnikov, *Appl. Catal. A Gen.* 378 (2010) 11–18.
- [10] M. Massa, A. Andersson, E. Finocchio, G. Busca, F. Lenrick, L.R. Wallenberg, *J. Catal.* 297 (2013) 93–109.
- [11] E. Tsukuda, S. Sato, R. Takahashi, T. Sodesawa, *Catal. Commun.* 8 (2007) 1349–1353.
- [12] J.P. Lourenço, M.I. Macedo, A. Fernandes, *Catal. Commun.* 19 (2012).
- [13] Y. Choi, H. Park, Y.S. Yun, J. Yi, *ChemSusChem.* 8 (2015) 974–979.
- [14] S.-H. Chai, H.-P. Wang, Y. Liang, B.-Q. Xu, *Green Chem.* 9 (2007) 1130.
- [15] A. Fernandes, M.F. Ribeiro, J.P. Lourenço, *Catal. Commun.* 95 (2017) 16–20.
- [16] H.H. Zhang, Z. Hu, L. Huang, H.H. Zhang, K. Song, L. Wang, Z. Shi, J. Ma, Y. Zhuang, W. Shen, Y. Zhang, H. Xu, Y. Tang, *ACS Catal.* 5 (2015) 2548–2558.
- [17] G. Sánchez, B.Z. Dlugogorski, E.M. Kennedy, M. Stockenhuber, *Appl. Catal. A Gen.* 509 (2016) 130–142.
- [18] T. Yoshikawa, T. Tago, A. Nakamura, A. Konaka, M. Mukaida, T. Masuda, *Res. Chem. Intermed.* 37 (2011) 1247–1256.
- [19] A. Ulgen, W.F. Hoelderich, *Appl. Catal. A Gen.* 400 (2011) 34–38.
- [20] J. Yi, S. Liu, M.M. Abu-Omar, *ChemSusChem.* 5 (2012) 1401–1404.
- [21] G. Sánchez, J. Friggieri, C. Keast, M. Drewery, B.Z. Dlugogorski, E. Kennedy, M. Stockenhuber, *Appl. Catal. B Environ.* 152–153 (2014) 117–128.
- [22] L.G. Possato, W.H. Cassinelli, T. Garetto, S.H. Pulcinelli, C. V. Santilli, L. Martins, *Appl. Catal. A Gen.* 492 (2015) 243–251.
- [23] A.R. Petersen, L.B. Nielsen, J.R. Dethlefsen, P. Fristrup, *ChemCatChem.* 10 (2018) 769–778.
- [24] J.P. Lourenço, A. Fernandes, C. Henriques, M.F. Ribeiro, *Microporous Mesoporous Mater.* 94 (2006) 56–65.
- [25] G. Catana, R.R. Rao, B.M. Weckhuysen, P. Van Der Voort, E. Vansant, R.A. Schoonheydt, *J. Phys. Chem. B.* 102 (1998) 8005–8012.
- [26] R. Bulánek, L. Čapek, M. Setnička, P. Čičmanec, *J. Phys. Chem. C.* 115 (2011) 12430–12438.
- [27] M. Wark, M. Koch, A. Brückner, W. Grünert, *J. Chem. Soc. - Faraday Trans.* 94 (1998) 2033–2041.
- [28] Y. Gu, N. Cui, Q. Yu, C. Li, Q. Cui, *Appl. Catal. A Gen.* 429–430 (2012) 9–16.
- [29] M. Guisnet, P. Magnoux, *Catal. Today.* 36 (1997) 477–483.
- [30] F.J. Maldonado, T. Bècue, J.M. Silva, M.F. Ribeiro, P. Massiani, M. Kermarec, *J. Catal.* 351 (2000) 342–351.

- [31] G.M. Lari, Z. Chen, C. Mondelli, J. Pérez-Ramírez, *ChemCatChem*. 9 (2017) 2195–2202.
- [32] Y. Liu, H. Tüysüz, C.-J. Jia, M. Schwickardi, R. Rinaldi, A.-H. Lu, W. Schmidt, F. Schüth, *Chem. Commun.* 46 (2010) 1238.

ACCEPTED MANUSCRIPT

Figure Captions

Figure 1. UV-Vis spectra of BEA/V (a), BEA/Cs/V (b) and commercial V_2O_5 (c).

Figure 2. Conversion of glycerol over BEA (●), BEA/V (■) and BEA/Cs/V (▲).

Figure 3. Selectivity towards reaction products over BEA: acrolein (●), hydroxyacetone (■), acetaldehyde (▲) and allyl alcohol (◆).

Figure 4. Heat profiles for the oxidation of coke of modified and non-modified BEA catalysts: sample BEA/V (a), sample BEA/Cs/V (b) and sample BEA (c).

Figure 5. Selectivity towards reaction products over BEA/V (A) and BEA/Cs/V (B): acrolein (●), hydroxyacetone (■), acetaldehyde (▲) and allyl alcohol (◆).

ACCEPTED MANUSCRIPT

Table 1. Chemical, acidic and textural properties of the prepared samples.

Sample	V (wt.%)	Cs (wt.%)	Acid sites ^a ($\mu\text{mol.g}^{-1}$)			Textural properties	
			Lewis ^b	Brönsted		S_{BET} ($\text{m}^2.\text{g}^{-1}$)	V_{mic}^c ($\text{cm}^3.\text{g}^{-1}$)
BEA	--	--	322	264		638	0.173
BEA/V	4.1	--	215	191		534	0.146
BEA/Cs/V	3.4	7.4	58	63		496	0.128

(a) measured at 150 °C.

(b) taking into consideration the bands at 1450 and 1455 cm^{-1} for the samples BEA/V and BEA/Cs/V.

(c) measured using *t*-plot method.

Highlights

- A one-pass conversion of glycerol to Allyl alcohol was achieved over a zeolite-based catalyst
- Modification of beta zeolite with Cs and V increases the selectivity towards allyl alcohol
- BEA/Cs/V recovers the catalytic activity and selectivity after a regeneration procedure

ACCEPTED MANUSCRIPT

Graphical abstract

ACCEPTED MANUSCRIPT

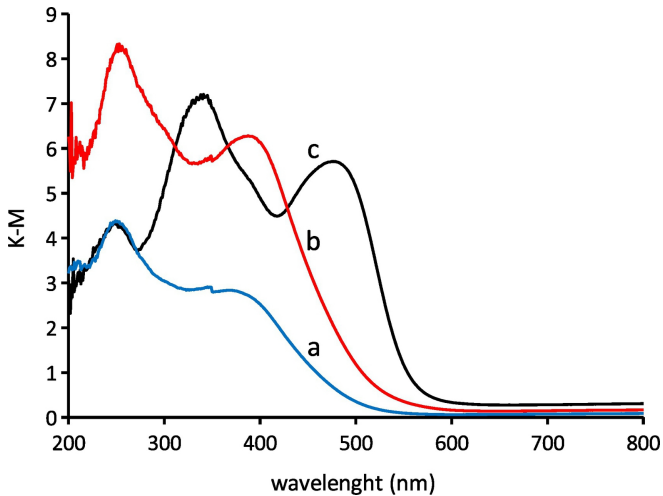


Figure 1

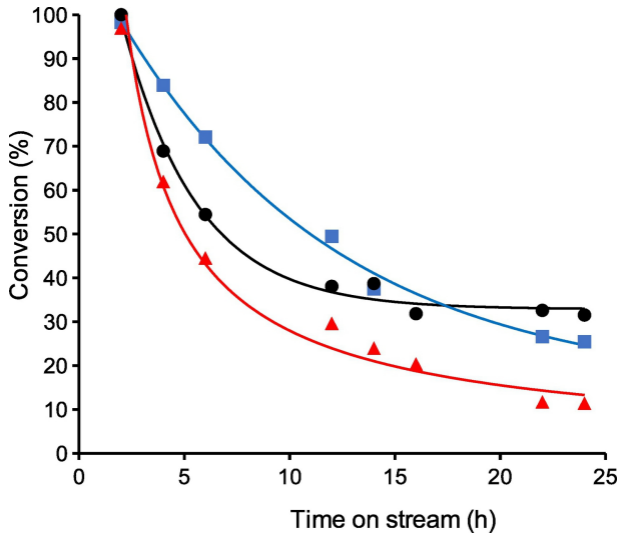


Figure 2

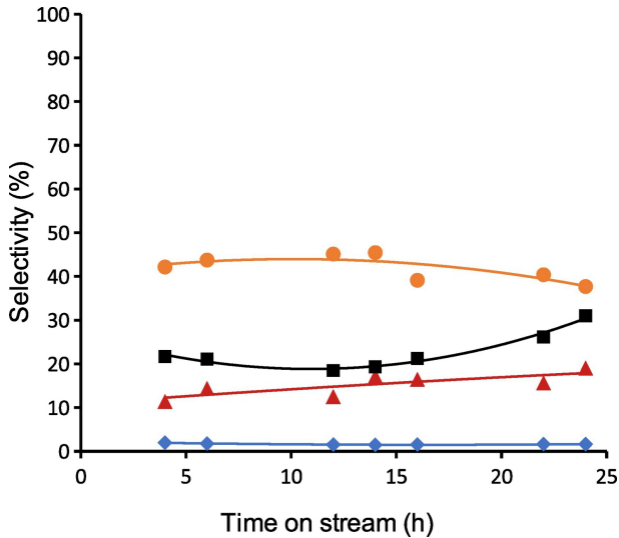


Figure 3

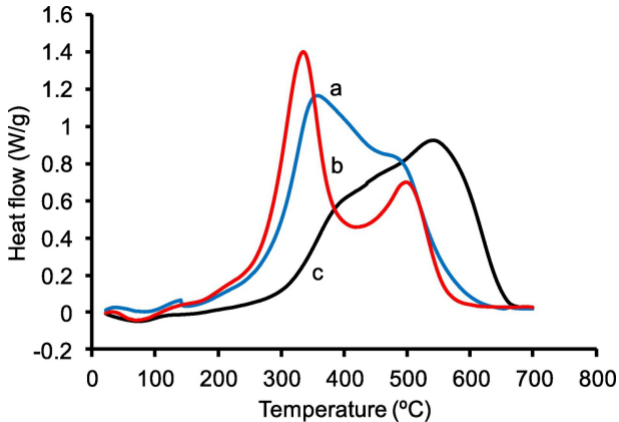


Figure 4

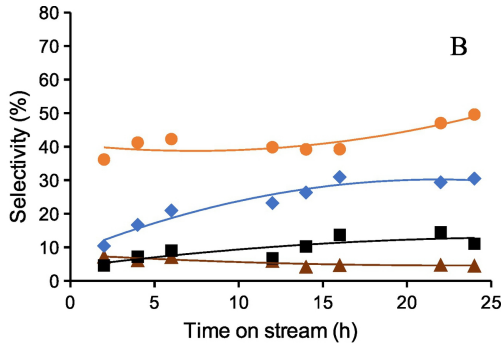
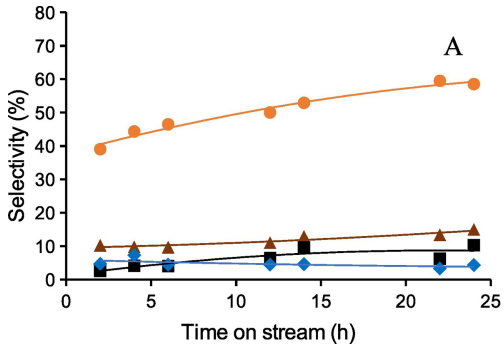


Figure 5